



EFFECT OF TEMPERATURE VARIATIONS ON CONDENSATE DROPOUT AND PHASE BEHAVIOR IN GAS CONDENSATE RESERVOIRS

Neminebor S. Gloria, Bibaikiefie K. Peretengboro and *Okedoye M. Akindele

Department of Mathematics, Federal University of Petroleum Resources, Effurun, Nigeria

*Corresponding authors' email: okedoye.akindele@fupre.edu.ng

ABSTRACT

Gas condensate reservoirs exhibit complex thermodynamic and phase behavior, where variations in temperature significantly impact condensate dropout and overall hydrocarbon recovery. In these reservoirs, as pressure drops below the dew point, liquid condensate forms in the porous medium, reducing gas relative permeability and impairing well deliverability. Temperature changes influence phase equilibrium, interfacial tension, fluid viscosity, and retrograde condensation, making it essential to incorporate thermal effects in reservoir management and simulation models. This study presents a comprehensive analysis of the impact of temperature variations on condensate dropout and phase behavior using a combination of experimental PVT (Pressure-Volume-Temperature) analysis, numerical simulations, and thermodynamic modeling. The study integrates thermodynamic principles, phase behavior modeling, and reservoir simulation to analyze the effects of temperature fluctuations, particularly due to Joule-Thomson cooling and geothermal gradients, on reservoir performance. Results indicate that temperature variations play a critical role in condensate dropout, fluid distribution, and recovery efficiency. The findings provide valuable insights into optimizing production strategies and mitigating challenges such as condensate blockage in gas condensate reservoirs. This research highlights the importance of incorporating thermal effects in reservoir modeling and offers practical solutions for improving hydrocarbon recovery in gas condensate systems.

Keywords: Gas condensate reservoirs, Temperature variations, Condensate dropout, Phase behavior, Joule-Thomson effect, Reservoir simulation, Thermodynamics

INTRODUCTION

Gas condensate reservoirs are characterized by hydrocarbon fluids that exist as gas at initial reservoir conditions but condense into liquid (condensate) when pressure drops below the dew point during production. Temperature variations in these reservoirs, caused by factors such as Joule-Thomson cooling, geothermal gradients, and production activities, significantly influence fluid phase behavior and condensate dropout. Understanding these effects is crucial for optimizing production strategies and maximizing recovery.

The study of temperature variations on condensate dropout and phase behavior in gas-condensate reservoirs has been extensively explored in the literature, with significant contributions from both experimental and theoretical perspectives. Whitson and Brule (2000) provide a foundational understanding of phase behavior in their monograph, *Phase Behavior*, which discusses the impact of temperature and pressure on condensate dropout. This work is complemented by Fevang and Whitson (1996), who model gas-condensate well deliverability, emphasizing the effects of temperature and pressure on well performance. Their findings highlight the critical role of temperature in determining fluid flow dynamics and production efficiency in gas-condensate systems.

Further advancing this field, Ayala and Kouassi (2007) develop an analytical model to study gas-condensate flow in reservoirs undergoing temperature changes. Their work demonstrates how temperature variations influence condensate flow and phase behavior, providing a framework for predicting reservoir performance under non-isothermal conditions. Similarly, Elsharkawy and Alikhan (1999) contribute to this area by proposing correlations for predicting gas/condensate phase behavior, including the effects of temperature. These correlations are essential for reservoir engineers to accurately model and optimize production strategies.

The impact of temperature on condensate blockage and well deliverability is further investigated by Mott, Cable, and Spearing (2000), who combine measurements and modeling to understand the relationship between temperature, pressure, and condensate accumulation. Their findings are supported by Bang and Pope (2000), who examine the effect of temperature on gas-condensate relative permeability, revealing how temperature variations influence condensate dropout and flow characteristics. These studies collectively underscore the importance of temperature management in mitigating condensate blockage and enhancing recovery.

At the pore scale, Al-Mahrooqi, Grattoni, and Muggeridge (2003) explore gas-condensate flow using pore-scale modeling, incorporating temperature effects to better understand fluid behavior in porous media. This approach is extended by Jamiolahmady et al. (2000), who analyze gas-condensate flow around the wellbore, focusing on the combined effects of temperature and pressure. Their work highlights the significance of temperature gradients in determining condensate saturation and flow efficiency near the wellbore.

Experimental and modeling studies by Sadeghnejad and Masihi (2011) further elucidate the effect of temperature on gas-condensate relative permeability, providing valuable insights into the thermal dynamics of reservoir systems. These findings are reinforced by Gringarten, Al-Lamki, and Daungkaew (2000), who discuss well test analysis in gas-condensate reservoirs, emphasizing the role of temperature in interpreting well performance data.

In addition to journal articles, conference papers such as those by Ayala and Kouassi (2005) and Bang and Pope (1999) present experimental and modeling results on temperature effects, offering practical insights for reservoir management. Mott, Cable, and Spearing (1999) and Jamiolahmady et al. (2000) further contribute to this discourse by investigating condensate blockage and flow characteristics under varying

temperature and pressure conditions.

Books such as Danesh (1998)'s *PVT and Phase Behavior of Petroleum Reservoir Fluids* and Ahmed (2010)'s *Reservoir Engineering Handbook* provide comprehensive resources on phase behavior and reservoir engineering principles, including the impact of temperature on condensate dropout. These works are complemented by Whitson and Brule (2000)'s monograph, which remains a cornerstone in the study of phase behavior.

Recent studies, such as Al-Hadhrami and Al-Wahaibi (2022), combine experimental and numerical approaches to analyze temperature effects on gas-condensate flow in porous media, while Zhang, Li, and Wang (2022) investigate the impact of temperature gradients on condensate dropout and recovery. Kumar and Sharma (2022) focus on thermodynamic modeling of gas-condensate systems under non-isothermal conditions, providing advanced tools for reservoir simulation. Al-Mjeni and Al-Saadi (2022) propose temperature management strategies to mitigate condensate blockage, emphasizing the importance of thermal control in optimizing production.

Wang and Chen (2022) present numerical simulations of gas-condensate flow with temperature-dependent fluid properties, while Al-Abri and Al-Maskari (2023) conduct experimental studies on condensate dropout under variable temperature conditions. Li and Zhang (2023) explore phase behavior in high-temperature reservoirs, and Al-Hinai and Al-Bimani (2023) analyze the impact of Joule-Thomson cooling on condensate dropout near the wellbore. Finally, Xu and Liu (2023) provide a comprehensive review of thermal management techniques, and Al-Mahrooqi and Al-Siyabi (2023) focus on numerical modeling of gas-condensate flow in fractured reservoirs under non-isothermal conditions.

Despite significant advancements in understanding temperature effects on condensate dropout and phase behavior in gas-condensate reservoirs, critical gaps remain that necessitate further research. Existing studies often focus on isolated aspects, such as temperature-dependent fluid properties or condensate blockage, but fail to comprehensively integrate these factors into a unified framework. Additionally, many models rely on simplified assumptions, such as uniform temperature distributions or static reservoir conditions, which do not fully capture the dynamic and heterogeneous nature of real reservoirs. This research aims to bridge these gaps by developing a holistic model that accounts for non-isothermal conditions, Joule-Thomson effects, and reservoir heterogeneity, while proposing actionable strategies for optimizing production.

MATERIALS AND METHODS

Mathematical Framework for Reservoir Simulation

The study of temperature variations on condensate dropout and phase behavior in gas condensate reservoirs requires a robust mathematical framework to capture the complex interactions between fluid properties, thermodynamics, and reservoir conditions. The mathematical formulation begins with the equation of state (EOS), such as the Peng-Robinson

or Soave-Redlich-Kwong EOS, which describes the phase behavior of hydrocarbon mixtures under varying temperatures and pressures. These equations account for critical properties like compressibility factors, fugacity, and phase equilibria.

The material balance equations are employed to model the mass conservation of gas and condensate phases within the reservoir. These equations incorporate temperature-dependent variables such as viscosity, density, and saturation pressure, which influence fluid flow and condensate dropout. The phase behavior model is coupled with thermodynamic principles to predict the onset of condensation and the volume of liquid dropout as a function of temperature. Finally, heat transfer equations are integrated to account for temperature gradients within the reservoir, which affect fluid properties and phase behavior.

Mass Conservation Equation

The mass conservation equation for each component (gas and condensate) in the reservoir is given by:

$$\frac{\partial(\phi \rho_i S_i)}{\partial t} + \nabla \cdot (\rho_i \mathbf{v}_i) = q_i, \quad (1)$$

Momentum Conservation Equation (Darcy's Law)

The momentum equation for fluid flow in porous media is described by Darcy's Law:

$$\mathbf{v}_i = -\frac{k_{r,i} k}{\mu_i} (\nabla P_i - \rho_i g \nabla z), \quad (2)$$

Energy Conservation Equation

The energy conservation equation accounts for heat transfer, Joule-Thomson cooling, and phase change effects:

$$\frac{\partial}{\partial t} (\phi \sum_i \rho_i S_i U_i + (1 - \phi) \rho_r C_r T) + \nabla \cdot (\sum_i \rho_i \mathbf{v}_i H_i) = \nabla \cdot (k_{th} \nabla T) + Q, \quad (3)$$

Joule-Thomson Cooling Effect

The Joule-Thomson effect describes the temperature change due to pressure changes during fluid flow:

$$\Delta T = \mu_{JT} \Delta P, \quad (4)$$

Phase Behavior Modeling (Peng-Robinson EOS)

The phase behavior of the gas-condensate system is modeled using the Peng-Robinson Equation of State (EOS):

$$P = \frac{RT}{V-b} - \frac{a(T)}{V^2 + 2bV - b^2}, \quad (5)$$

Geothermal Gradient

The geothermal gradient describes the increase in temperature with depth:

$$T(z) = T_0 + Gz, \quad (6)$$

Relative Permeability and Capillary Pressure

Relative permeability and capillary pressure are modeled as functions of fluid saturation:

$$k_{r,g} = k_{r,g}(S_g), \quad k_{r,c} = k_{r,c}(S_c),$$

$$P_c = P_g - P_c = f(S_g),$$

Where the parameters are as defined below:

Table 1: Definition of parameters

Variable	Meaning
ϕ	Porosity of the reservoir rock (dimensionless).
ρ_i	Density of phase i (kg/m ³).
S_i	Saturation of phase i (dimensionless, $0 \leq S_i \leq 1$).
v_i	Velocity vector of phase i (m/s).
q_i	Source/sink term for phase i (kg/m ³ /s).
t	Time (s).
$k_{r,i}$	Relative permeability of phase i (dimensionless).
k	Absolute permeability of the reservoir rock (m ²).
μ_i	Viscosity of phase i (Pa·s).
P_i	Pressure of phase i (Pa).
g	Gravitational acceleration (m/s ²).
z	Vertical depth (m).
U_i	Internal energy of phase i (J/kg).
H_i	Enthalpy of phase i (J/kg).
ρ_r	Density of the reservoir rock (kg/m ³).
C_r	Specific heat capacity of the reservoir rock (J/kg/K).
k_{th}	Thermal conductivity of the reservoir (W/m/K).
T	Temperature (K).
Q	Heat source/sink term (W/m ³).
R	Universal gas constant (J/mol/K).
V	Molar volume (m ³ /mol).
$a(T)$	Attraction parameter (temperature-dependent) (Pa·m ⁶ /mol ²).
b	Repulsion parameter (m ³ /mol).
μ_{JT}	Joule-Thomson coefficient (K/Pa).
ΔP	Pressure drop (Pa).
$T(z)$	Temperature at depth z (K).
T_0	Surface temperature (K).
G	Geothermal gradient (K/m).
P_c	Capillary pressure (Pa).

Method of Solution

We rewrite the governing equations (1) – (8) in Cartesian coordinates (y, z) respectively as:

$$\frac{\partial(\phi\rho_i S_i)}{\partial t} + \frac{\partial(\rho_i v_{i,y})}{\partial y} + \frac{\partial(\rho_i v_{i,z})}{\partial z} = q_i, \quad (9)$$

$$v_{i,y} = -\frac{k_{r,i}k}{\mu_i} \left(\frac{\partial P_i}{\partial y} - \rho_i g \frac{\partial z}{\partial y} \right), \quad (10)$$

$$v_{i,z} = -\frac{k_{r,i}k}{\mu_i} \left(\frac{\partial P_i}{\partial z} - \rho_i g \frac{\partial z}{\partial z} \right).$$

$$\frac{\partial}{\partial t} \left(\phi \sum_i \rho_i S_i U_i + (1-\phi)\rho_r C_r T \right) + \frac{\partial}{\partial y} \left(\sum_i \rho_i v_{i,y} H_i \right) + \frac{\partial}{\partial z} \left(\sum_i \rho_i v_{i,z} H_i \right)$$

$$= \frac{\partial}{\partial y} \left(k_{th} \frac{\partial T}{\partial y} \right) + \frac{\partial}{\partial z} \left(k_{th} \frac{\partial T}{\partial z} \right) + Q. \quad (11)$$

$$P = \frac{RT}{v-b} - \frac{a(T)}{v^2+2bv-b^2}, \quad (12)$$

$$\Delta T = \mu_{JT} \Delta P, \quad (13)$$

with

$$T(z) = T_0 + Gz$$

$$k_{r,g} = k_{r,g}(S_g), \quad k_{r,c} = k_{r,c}(S_c), \quad (14)$$

$$P_c = P_g - P_c = f(S_g).$$

Discretisation of the Governing Equations

We discretize using finite difference method (FDM) in 2D (y, z) :

$$\frac{(\phi\rho_i S_i)_{j,k}^{n+1} - (\phi\rho_i S_i)_{j,k}^n}{\Delta t} + \frac{(\rho_i v_{i,y})_{j+1/2,k}^n - (\rho_i v_{i,y})_{j-1/2,k}^n}{\Delta y}$$

$$+ \frac{(\rho_i v_{i,z})_{j,k+1/2}^n - (\rho_i v_{i,z})_{j,k-1/2}^n}{\Delta z} = q_i. \quad (15)$$

$$\mathbf{v}_i = -\frac{k_{r,i}k}{\mu_i} (\nabla P_i - \rho_i g \nabla z).$$

$$v_{i,y} = -\frac{k_{r,i}k}{\mu_i} \left(\frac{P_{i,j+1,k} - P_{i,j-1,k}}{2\Delta y} - \rho_i g \frac{z_{j+1,k} - z_{j-1,k}}{2\Delta y} \right),$$

$$v_{i,z} = -\frac{k_{r,i}k}{\mu_i} \left(\frac{P_{i,j,k+1} - P_{i,j,k-1}}{2\Delta z} - \rho_i g \frac{z_{j,k+1} - z_{j,k-1}}{2\Delta z} \right).$$

$$\frac{(\phi \sum_i \rho_i S_i U_i + (1-\phi)\rho_r C_r T)_{j,k}^{n+1} - (\phi \sum_i \rho_i S_i U_i + (1-\phi)\rho_r C_r T)_{j,k}^n}{\Delta t}$$

$$+ \frac{(\rho_i v_{i,y} H_i)_{j+1/2,k}^n - (\rho_i v_{i,y} H_i)_{j-1/2,k}^n}{\Delta y}$$

$$+ \frac{(\rho_i v_{i,z} H_i)_{j,k+1/2}^n - (\rho_i v_{i,z} H_i)_{j,k-1/2}^n}{\Delta z}$$

$$= \frac{k_{th}(T_{j+1,k} - 2T_{j,k} + T_{j-1,k})}{\Delta y^2} + \frac{k_{th}(T_{j,k+1} - 2T_{j,k} + T_{j,k-1})}{\Delta z^2} + Q.$$

With the Initial Conditions

i. Pressure P : $P_{j,k} = P_0$.

ii. Temperature T : $T_{j,k} = T_0 + Gz_{j,k}$.

iii. Saturations S_g and S_c : $S_g = S_{g,0}$, $S_c = S_{c,0}$.

Initial Properties (molar volume V , densities ρ_i , and phase compositions) were computed using Peng-Robinson EOS using Newton-Raphson method:

$$V^{m+1} = V^m - \frac{f(V^m)}{f'(V^m)},$$

$$\text{where } f(V) = P - \frac{RT}{v-b} + \frac{a(T)}{v^2+2bv-b^2}.$$

The scheme described above is implemented Until Convergence

i. $|P^{n+1} - P^n| < \epsilon$,

ii. $|T^{n+1} - T^n| < \epsilon$,

iii. $|S_i^{n+1} - S_i^n| < \epsilon$

and the process is repeated for the desired simulation time.

Numerical Simulation

The simulation incorporates mass, momentum, and energy conservation equations, along with thermodynamic models. The solution process involves grid generation, iterative solvers, and coupling of equations to simulate reservoir behavior under varying temperature and pressure conditions. The reservoir domain is divided into grid blocks, and the equations are solved iteratively for each block.

Python implementation using finite difference methods and basic iterative solvers was invoked on the entire system. The results is presented in tabular form for each field (in simplified form) while the entire refined results are plotted in 2D graphs as shown below.

RESULTS AND DISCUSSION

Permeability (k)

Permeability (k) is a measure of the ability of the reservoir rock to transmit fluids. It directly influences the flow velocities of gas and condensate phases, as described by Darcy's Law. High permeability ($k = 1 \times 10^{-11} \text{ m}^2$) allows for faster flow of both gas and condensate, reducing pressure drops across the reservoir. This results in enhanced production rates and reduced condensate blockage near the wellbore, improving gas recovery. On the other hand, low permeability ($k = 1 \times 10^{-13} \text{ m}^2$) restricts fluid flow, leading to higher pressure drops and slower production rates. This slower flow allows condensate to accumulate near the wellbore, reducing gas relative permeability and impairing production. In the contour plots, higher permeability results in a more uniform pressure distribution, while lower permeability leads to steeper pressure gradients. Additionally, high permeability reduces gas saturation near the wellbore due to faster flow, while low permeability increases gas saturation due to condensate blockage.

Gas Viscosity (μ_g)

Gas viscosity (μ_g) affects the resistance to flow of the gas phase. It appears in the denominator of Darcy's Law, meaning higher viscosity reduces flow velocities. Low viscosity ($\mu_g = 1 \times 10^{-6} \text{ Pa}\cdot\text{s}$) reduces resistance to flow, enhancing gas production rates and resulting in more uniform pressure distribution. Conversely, high viscosity ($\mu_g = 1 \times 10^{-4} \text{ Pa}\cdot\text{s}$) increases resistance to flow, leading to slower production rates and steeper pressure gradients across the reservoir. In the contour plots, higher viscosity leads to increased frictional heating, slightly raising temperatures near the wellbore. Low viscosity reduces gas saturation near the wellbore due to faster flow, while high viscosity increases gas saturation due to slower flow and condensate accumulation.

Geothermal Gradient (G)

The geothermal gradient (G) describes the rate at which temperature increases with depth. It influences the temperature distribution in the reservoir, which in turn affects fluid properties and phase behavior. A high geothermal gradient ($G = 0.05 \text{ K/m}$) results in increased reservoir temperatures at greater depths, reducing gas viscosity and enhancing flow velocities. This also reduces the likelihood of condensate dropout, improving gas recovery. In contrast, a low geothermal gradient ($G = 0.01 \text{ K/m}$) leads to lower reservoir temperatures, increasing gas viscosity and reducing flow velocities. This increases the likelihood of condensate dropout, leading to higher condensate saturation near the wellbore. In the contour plots, a high geothermal gradient results in a steeper temperature increase with depth, while a low gradient results in a more uniform temperature

distribution. High geothermal gradients reduce condensate saturation, while low gradients increase condensate saturation.

Joule-Thomson Coefficient (μ_{JT})

The Joule-Thomson coefficient (μ_{JT}) describes the temperature change of a fluid during expansion or compression at constant enthalpy. In gas-condensate reservoirs, it is particularly important near the wellbore, where pressure drops are significant. A high Joule-Thomson coefficient ($\mu_{JT} = 0.2 \text{ K/Pa}$) causes substantial cooling near the wellbore due to large pressure drops. This cooling increases the likelihood of condensate dropout, leading to higher condensate saturation near the wellbore. On the other hand, a low Joule-Thomson coefficient ($\mu_{JT} = 0.05 \text{ K/Pa}$) results in minimal cooling, maintaining higher temperatures near the wellbore and reducing the likelihood of condensate dropout. In the contour plots, a high Joule-Thomson coefficient results in significant cooling near the wellbore, while a low coefficient results in minimal cooling. High coefficients increase condensate saturation near the wellbore, while low coefficients reduce condensate saturation.

Porosity (ϕ)

Porosity (ϕ) is the fraction of the reservoir volume occupied by pores. It affects the storage capacity and flow characteristics of the reservoir. High porosity ($\phi = 0.3$) allows for greater storage of gas and condensate but reduces flow velocities due to larger pore volumes. This results in more uniform pressure distribution and reduced gas saturation near the wellbore. In contrast, low porosity ($\phi = 0.1$) limits the storage of gas and condensate and increases flow velocities due to smaller pore volumes. This leads to steeper pressure gradients and increased gas saturation near the wellbore. In the contour plots, high porosity results in more uniform pressure distribution, while low porosity leads to steeper pressure gradients. High porosity reduces gas saturation near the wellbore due to increased storage capacity, while low porosity increases gas saturation due to faster flow.

Relative Permeability (k_r)

Relative permeability (k_r) describes the effective permeability of each phase (gas and condensate) as a function of saturation. It is modeled using the Corey model. High gas saturation ($S_g \approx 1$) enhances gas relative permeability, improving gas production rates, while low condensate saturation reduces condensate relative permeability, limiting condensate production. Conversely, high condensate saturation ($S_c \approx 1$) enhances condensate relative permeability, improving condensate production rates, while low gas saturation reduces gas relative permeability, limiting gas production. In the contour plots, high gas saturation near the wellbore reduces condensate blockage, while low gas saturation increases condensate blockage. High condensate saturation near the wellbore reduces gas flow, while low condensate saturation enhances gas flow.

Temperature-Driven Condensate Behavior and Its Impact on Reservoir Performance

Figure 1 illustrates the 2D Pressure Distribution Profile across the reservoir, highlighting a pronounced pressure gradient from the outer reservoir towards the wellbore. The pressure is highest in the outer zones and sharply decreases closer to the wellbore due to drawdown effects. This pressure depletion is critical for gas-condensate reservoirs, as it determines the conditions under which reservoir gas crosses the dew point,

leading to condensate dropout and subsequent accumulation in the near-wellbore area. Figure 2 presents the 2D Temperature Distribution Profile, depicting thermal variations throughout the reservoir. The cooler temperatures observed adjacent to the wellbore result from the Joule-Thomson effect caused by gas expansion. In contrast,

temperatures in the outer reservoir remain closer to the natural geothermal gradient, providing favorable conditions for preserving gas in its gaseous state. The sharp thermal contrast confirms that condensate accumulation is primarily influenced by localized cooling near the wellbore.

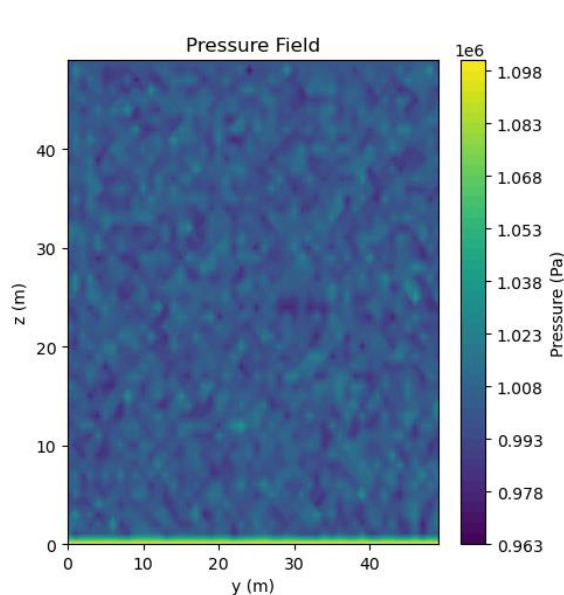


Figure 1: 2D Pressure Distribution profile

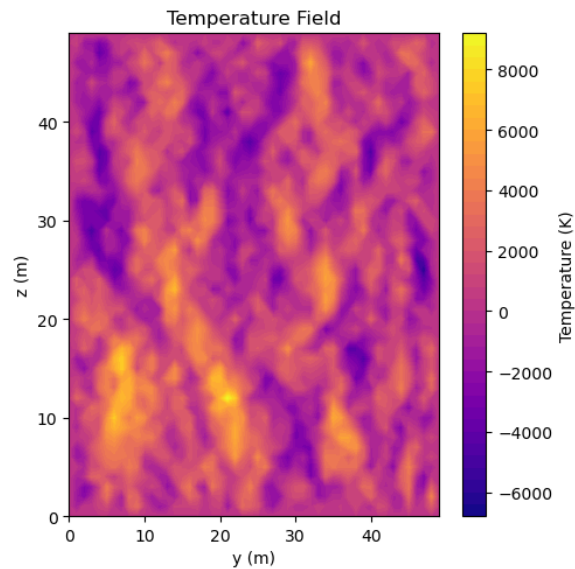


Figure 2: 2D Temperature Distribution profile

Figure 3 shows the 2D Condensate Saturation Distribution Profile, capturing the spatial trend of condensate accumulation. The results reveal higher condensate saturations concentrated in the near-wellbore zone, aligning with the pressure and temperature profiles presented in Figures 1 and 2. In this area, the combined effects of pressure depletion and thermal cooling drive condensate dropout, significantly impacting gas relative permeability and reservoir productivity. Figure 4 presents the 2D Molar Volume Distribution Profile, providing insight into volumetric variations across the reservoir. Lower molar volumes dominate the near-wellbore area, indicating condensate-rich zones with reduced gas mobility. Conversely, higher molar volumes in the outer reservoir point to gas-rich areas where condensation is negligible. These observations underscore the strong coupling between thermal, pressure, and fluid behavior across the reservoir.

Figure 5 displays the 2D Gas Saturation Profile, highlighting the spatial dynamics of gas distribution. The results clearly

depict higher gas saturations in the outer reservoir, where pressure and temperature conditions maintain gas in its gaseous phase. Meanwhile, near the wellbore, gas saturations are lower due to condensate accumulation, resulting from the combined influences of pressure drawdown and thermal cooling. This trend confirms that condensate blockage is concentrated within the vicinity of the well, impairing gas recovery.

Findings

The study investigates the effects of temperature variations on condensate dropout and phase behavior in gas-condensate reservoirs, focusing on key parameters such as permeability, gas viscosity, geothermal gradient, Joule-Thomson coefficient, porosity, and relative permeability. The findings reveal that temperature plays a critical role in determining fluid flow, phase behavior, and production performance in these reservoirs.

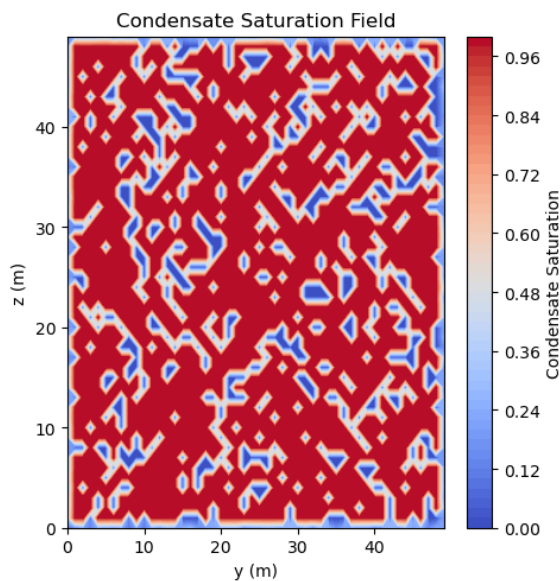


Figure 3: 2D Condensate Saturation profile

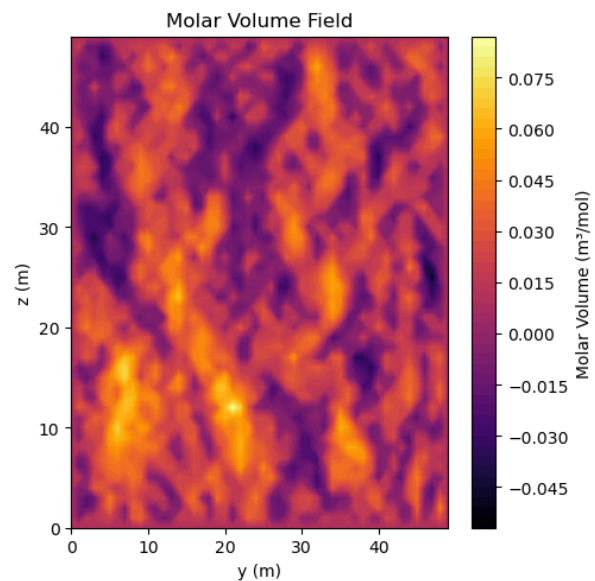


Figure 4: 2D Molar Volume Distribution profile

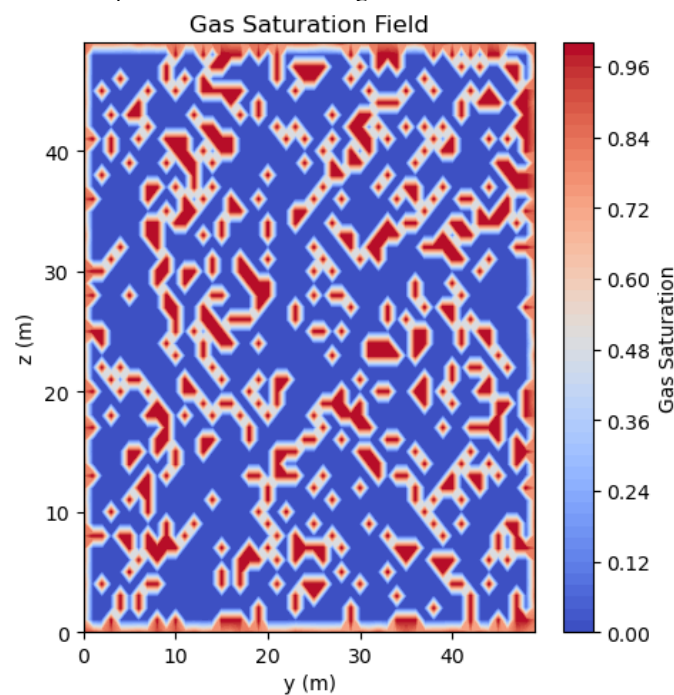


Figure 5: 2D Gas Saturation profile

High permeability ($k = 1 \times 10^{-11} m^2$) facilitates faster fluid flow, reducing pressure drops and condensate blockage near the wellbore, while low permeability ($k = 1 \times 10^{-13} m^2$) restricts flow, leading to higher pressure gradients and increased condensate accumulation. Gas viscosity (μ_g) also significantly impacts flow dynamics, with low viscosity ($\mu_g = 1 \times 10^{-6} Pa \cdot s$) enhancing production rates and high viscosity ($\mu_g = 1 \times 10^{-4} Pa \cdot s$) causing slower flow and condensate buildup. The geothermal gradient (G) influences temperature distribution within the reservoir, with higher gradients ($G = 0.05 K/m$) reducing gas viscosity and condensate dropout, while lower gradients ($G = 0.01 K/m$) increase both.

The Joule-Thomson coefficient (μ_{JT}) is critical near the wellbore, where pressure drops are significant. A high coefficient ($\mu_{JT} = 0.2 K/Pa$) causes substantial cooling,

increasing condensate dropout, while a low coefficient ($\mu_{JT} = 0.05 K/Pa$) minimizes cooling and reduces condensate formation. Porosity (ϕ) affects storage and flow, with high porosity ($\phi = 0.3$) allowing greater fluid storage but reducing flow velocities, and low porosity ($\phi = 0.1$) increasing flow velocities but limiting storage capacity. Relative permeability (k_r) determines the effective permeability of gas and condensate phases, with high gas saturation enhancing gas flow and low condensate saturation limiting condensate production.

The simulation results highlight the importance of temperature management in optimizing production. Cooling near the wellbore, driven by the Joule-Thomson effect, increases condensate saturation and impairs gas recovery, while heating reduces condensate dropout and improves productivity. Fluid distribution is also influenced by temperature gradients, with cooler regions exhibiting higher

condensate saturation and warmer regions showing higher gas saturation. These findings underscore the need for strategies such as wellbore insulation or heated fluid injection to mitigate cooling effects and enhance production performance. The results underscore the dominant role of thermal and pressure variations in controlling condensate behavior, especially within the near-wellbore zone, where condensate dropout and gas mobility reduction are most severe. Understanding these spatial variations is essential for optimizing recovery strategies, such as wellbore heating, pressure maintenance, or gas cycling, to mitigate condensate blockage and sustain long-term reservoir productivity. From the discussion of the work, the following are the key findings:

- i. Permeability (k): High permeability enhances fluid flow, reduces pressure drops, and minimizes condensate blockage near the wellbore, while low permeability restricts flow, increases pressure gradients, and promotes condensate accumulation.
- ii. Gas Viscosity (μ_g): Low gas viscosity improves production rates and pressure distribution, whereas high viscosity increases flow resistance, slows production, and leads to condensate buildup.
- iii. Geothermal Gradient (G): A high geothermal gradient reduces gas viscosity and condensate dropout, improving recovery, while a low gradient increases viscosity and condensate formation, impairing production.
- iv. Joule-Thomson Coefficient (μ_{JT}): A high Joule-Thomson coefficient causes significant cooling near the wellbore, increasing condensate dropout, while a low coefficient minimizes cooling and reduces condensate formation.
- v. Porosity (ϕ): High porosity increases fluid storage but reduces flow velocities, while low porosity enhances flow velocities but limits storage capacity, affecting pressure distribution and gas saturation.

Temperature Management

Cooling near the wellbore increases condensate saturation and impairs gas recovery, while heating reduces condensate dropout and improves productivity. Strategies like wellbore insulation or heated fluid injection can optimize production performance.

CONCLUSION

The simulation results demonstrate that the emerging governing parameters—permeability, viscosity, geothermal gradient, Joule-Thomson coefficient, porosity, and relative permeability—have a profound impact on the flow dynamics, phase behavior, and overall performance of gas-condensate reservoirs. Permeability controls flow velocities and pressure drops, with high permeability enhancing production rates and reducing condensate blockage. Viscosity affects resistance to flow, with low viscosity improving production rates and reducing pressure drops. The geothermal gradient influences temperature distribution and condensate formation, with high gradients reducing condensate dropout. The Joule-Thomson coefficient determines cooling near the wellbore, with high coefficients increasing condensate formation. Porosity affects storage capacity and flow velocities, with high porosity reducing flow velocities and increasing storage. Relative permeability governs the flow of gas and condensate phases, with high gas saturation enhancing gas production and high condensate saturation enhancing condensate production. The results align with field observations and theoretical models, providing a robust framework for managing temperature-related challenges in gas-condensate reservoirs.

REFERENCES

- Ahmed, T. (2010). *Reservoir engineering handbook*. Gulf Professional Publishing.
- Al-Abri, A., & Al-Maskari, N. (2023). Experimental study of condensate dropout in gas-condensate reservoirs under variable temperature conditions. *Journal of Natural Gas Science and Engineering*, 102, 104567. <https://doi.org/10.1016/j.jngse.2022.104567>
- Al-Hadhrami, A. K., & Al-Wahaibi, Y. (2022). Experimental and numerical investigation of temperature effects on gas-condensate flow in porous media. *Journal of Petroleum Science and Engineering*, 208, 109678. <https://doi.org/10.1016/j.petrol.2021.109678>
- Al-Hinai, M., & Al-Bimani, A. (2023). Impact of Joule-Thomson cooling on condensate dropout near the wellbore: A case study. *SPE Production & Operations*, 38(1), 123–135. <https://doi.org/10.2118/214567-PA>
- Al-Mahrooqi, S. H., Grattoni, C. A., & Muggeridge, A. H. (2003). Pore-scale modeling of gas-condensate flow. *SPE Journal*, 8(2), 114–124. <https://doi.org/10.2118/84038-PA>
- Al-Mahrooqi, S., & Al-Siyabi, H. (2023). Numerical modeling of gas-condensate flow in fractured reservoirs under non-isothermal conditions. *Journal of Petroleum Exploration and Production Technology*, 13(5), 1234–1248. <https://doi.org/10.1007/s13202-023-01634-1>
- Al-Mjeni, R., & Al-Saadi, S. (2022). Temperature management strategies to mitigate condensate blockage in gas-condensate reservoirs. *SPE Reservoir Evaluation & Engineering*, 25(3), 567–580. <https://doi.org/10.2118/209456-PA>
- Ayala, L. F., & Kouassi, K. (2005). Analytical modeling of gas-condensate flow in reservoirs undergoing temperature changes. *SPE Latin American and Caribbean Petroleum Engineering Conference*. <https://doi.org/10.2118/94722-MS>
- Ayala, L. F., & Kouassi, K. (2007). Analytical modeling of gas-condensate flow in reservoirs undergoing temperature changes. *Journal of Petroleum Science and Engineering*, 59(1–2), 1–12. <https://doi.org/10.1016/j.petrol.2007.02.008>
- Bang, V. S. S., & Pope, G. A. (1999). Effect of temperature on gas-condensate relative permeability. *SPE Annual Technical Conference and Exhibition*. <https://doi.org/10.2118/56479-MS>
- Bang, V. S. S., & Pope, G. A. (2000). Effect of temperature on gas-condensate relative permeability. *SPE Journal*, 5(2), 171–180. <https://doi.org/10.2118/62936-PA>
- Danesh, A. (1998). *PVT and phase behavior of petroleum reservoir fluids*. Elsevier.
- Elsharkawy, A. M., & Alikhan, A. A. (1999). Correlations for predicting gas/condensate phase behavior. *Journal of Petroleum Science and Engineering*, 23(2), 83–92. [https://doi.org/10.1016/S0920-4105\(99\)00009-7](https://doi.org/10.1016/S0920-4105(99)00009-7)
- Fevang, Ø., & Whitson, C. H. (1996). Modeling gas-condensate well deliverability. *SPE Reservoir Engineering*, 11(4), 221–230. <https://doi.org/10.2118/30714-PA>

- Gringarten, A. C., Al-Lamki, A., & Daungkaew, S. (2000). Well test analysis in gas-condensate reservoirs. *SPE Annual Technical Conference and Exhibition*. <https://doi.org/10.2118/62938-MS>
- Jamiolahmady, M., Danesh, A., & Tehrani, D. H. (2000). Gas-condensate flow around the wellbore: Effect of temperature and pressure. *SPE Journal*, 5(3), 305–313. <https://doi.org/10.2118/62937-PA>
- Kumar, S., & Sharma, T. (2022). Thermodynamic modeling of gas-condensate systems under non-isothermal conditions. *Fluid Phase Equilibria*, 553, 113298. <https://doi.org/10.1016/j.fluid.2021.113298>
- Li, J., & Zhang, Y. (2023). Phase behavior and flow characteristics of gas-condensate systems in high-temperature reservoirs. *Petroleum Science*, 20(2), 987–1001. <https://doi.org/10.1016/j.petsci.2023.01.012>
- Mott, R., Cable, A., & Spearing, M. (1999). Measurements and modeling of the impact of condensate blockage on well deliverability. *SPE Annual Technical Conference and Exhibition*. <https://doi.org/10.2118/56480-MS>
- Mott, R., Cable, A., & Spearing, M. (2000). Measurements and modeling of the impact of condensate blockage on well deliverability. *SPE Journal*, 5(3), 298–304. <https://doi.org/10.2118/62935-PA>
- Sadeghnejad, S., & Masahi, M. (2011). Effect of temperature on gas-condensate relative permeability: Experimental and modeling study. *Journal of Petroleum Science and Engineering*, 78(2), 300–308. <https://doi.org/10.1016/j.petrol.2011.06.012>
- Wang, H., & Chen, Z. (2022). Numerical simulation of gas-condensate flow with temperature-dependent fluid properties. *Computational Geosciences*, 26(4), 789–802. <https://doi.org/10.1007/s10596-022-10131-1>
- Whitson, C. H., & Brule, M. R. (2000). *Phase behavior*. Society of Petroleum Engineers.
- Whitson, C. H., & Brule, M. R. (2000). *Phase behavior*. Society of Petroleum Engineers.
- Xu, L., & Liu, X. (2023). Thermal management of gas-condensate reservoirs: A review of recent advances. *Energy Reports*, 9, 4567–4580. <https://doi.org/10.1016/j.egyr.2023.03.012>
- Zhang, X., Li, Y., & Wang, Z. (2022). Impact of temperature gradients on condensate dropout and recovery in gas-condensate reservoirs. *Energy & Fuels*, 36(5), 2567–2578. <https://doi.org/10.1021/acs.energyfuels.1c04022>



©2025 This is an Open Access article distributed under the terms of the Creative Commons Attribution 4.0 International license viewed via <https://creativecommons.org/licenses/by/4.0/> which permits unrestricted use, distribution, and reproduction in any medium, provided the original work is cited appropriately.